[CANCER RESEARCH 55, 1248–1254, March 15, 1995]

In Vitro and *in Vivo* ^{31}P Nuclear Magnetic Resonance Measurements of Metabolic Changes Post Radiation[1]

Umar Mahmood, Alan A. Alfieri, Douglas Ballon, Frank Traganos, and Jason A. Koutcher[2]

Departments of Medical Physics [U. M., A. A. A., D. B., J. A. K.], Radiology [D. B., J. A. K.], and Medicine [J. A. K.], Memorial Sloan-Kettering Cancer Center, and Cornell University Graduate School of Medical Sciences [U. M.], New York, New York 10021; The Cancer Research Institute, New York Medical College, Elmsford, New York 10523 [F. T.]; and Beth Israel Medical Center, New York, New York 10003 [A. A.]

ABSTRACT

Radiation-induced metabolic changes previously observed in tumors using phosphorus nuclear magnetic resonance spectroscopy include changes in the relative amounts of the phospholipid precursors phosphoethanolamine and phosphocholine, increases in membrane catabolites, and increases in energy status. To elucidate the degree to which these *in vivo* alterations are a result of intrinsic cellular changes *versus* radiation-induced systemic effects, the Radiation-Induced Fibrosarcoma-1 tumor model was studied before and over the course of 7 days after a single dose of 17 Gy. *In vivo* studies were performed with tumors implanted in C3H/He mice; *in vitro* studies used cells that were perfused in agarose gel threads after being grown, radiated, and maintained in monolayer. The statistically significant increases in the downfield component of the phosphomonoester peak, which consists primarily of phosphoethanolamine, compared to the upfield component, phosphocholine, were qualitatively similar *in vivo* and *in vitro* post radiation. Statistically significant increases in the membrane catabolite glycerophosphocholine, a phosphodiester, were also observed in both tumors and cell culture after irradiation, with a greater percentage change *in vitro*. This suggests that changes in the phosphomonoester and phosphodiester concentrations are primarily an intrinsic effect of radiation on cellular metabolism, modulated to a lesser degree by systemic effects. In contrast, the statistically significant increases in energy status after the 17-Gy dose showed markedly different temporal responses in the two systems. Therefore, energy status changes observed *in vivo* are due largely to systemic changes, such as changes in blood flow. Flow cytometry data obtained from the cultured cells showed a sustained increase in the G_2-M fraction starting at 24 h, the first time point measured after irradiation, which continued for the 7 days studied post radiation. These data indicate that the *in vivo* changes detected by nuclear magnetic resonance in phospholipid precursors and catabolites occur directly at the cellular level and may reflect cell death or growth inhibition after antineoplastic therapy.

INTRODUCTION

In vivo phosphorus nuclear magnetic resonance spectroscopy offers a noninvasive view of tumor physiology and alterations in metabolism created by therapy, both in patients and in experimental tumor model systems (1–7). *In vivo* systems are multicomponent in nature; antineoplastic therapy may alter one or more such components. Tumor cells may be directly affected by modification of DNA, proteins, energy status, and membranes among many possible therapeutic targets. Systemic changes may also affect these same targets indirectly, via alterations in the circulatory system, including changes in perfusion rate and pressure, and vascular damage; changes in hormonal levels; variation in levels of nutrients such as glucose and oxygen; and alterations in immune response. Knowledge of the underlying mechanisms of observed changes allows for more rational treatment design and therapeutic modality combinations.

Changes we have previously noted after tumor irradiation in the *in vivo* ^{31}P NMR[3] spectra of the murine MCa tumor model include increases in PME′, compared to the upfield component, phosphocholine; increases in the membrane catabolites seen in the phosphodiester region of the spectra; and increases in high-energy phosphates (1, 2, 8). PME′ is used instead of PE throughout this article to represent the downfield component of the PME peak, because it contains minor contributions from other compounds in addition to phosphoethanolamine in both the MCa and RIF-1 tumors.[4] To determine if these changes are direct cellular effects of radiation or if they are physiologically induced, a comparison of *in vitro* and *in vivo* models was necessary. Since the MCa tumor line could not be grown in cell culture, we have studied the RIF-1 fibrosarcoma both *in vivo* and *in vitro* after 17 Gy of radiation. Tumors were implanted on the feet of C3H/He mice and were followed serially over the course of 7 days after radiation for the *in vivo* studies. Cells were grown and radiated in monolayer, with data for each time point post radiation obtained from a different set of cells, for the *in vitro* studies. Cell cycle data from the cultured cells were also used to determine the relationship between metabolic and cell cycle changes.

The effects of radiation on the metabolic response of the RIF-1 tumor model have been studied previously *in vivo* (9–11) and *in vitro* (12). We undertook the current study because the increased spectral resolution obtained using susceptibility matching (13) allowed the resolution of the PME peak into two components for both *in vivo* and *in vitro* states. We present data showing changes in the PME and PDE resonances, which represent changes in phospholipid precursors and catabolites, not previously detected post radiation *in vivo* and *in vitro* for a single tumor model.

MATERIALS AND METHODS

***In Vivo* NMR.** RIF-1 tumors were maintained by alternate *in vivo* (flank) and *in vitro* passage, as recommended by Twentyman *et al.* (14). For the *in vivo* studies, a tumor cell inoculum of 0.01–0.02 ml was injected s.c. into the dorsum of the feet of male C3H/He mice (The Jackson Laboratory, Bar Harbor, ME) with a 26-gauge needle. Tumor volume was estimated as

$$V = \pi \frac{d_1 \times d_2 \times d_3}{6}$$

where d_1, d_2, and d_3 are three orthogonal diameters. Baseline tumor volumes ranged from 150 to 250 mm^3. The *in vivo* tumors were serially followed, with spectra obtained prior to radiation and at 1, 2, 4, and 7 days post treatment.

^{31}P NMR spectra were obtained at 81.03 MHz on a Bruker CSI 4.7-T magnet. The dorsal aspect of the foot was chosen as the inoculation site to minimize spectral contamination from adjacent tissues (15, 16). In order to

Received 9/9/94; accepted 1/17/95.

The costs of publication of this article were defrayed in part by the payment of page charges. This article must therefore be hereby marked *advertisement* in accordance with 18 U.S.C. Section 1734 solely to indicate this fact.

[1] This work was supported by Grants 5 PO1 CA 25842-14 and NIH CA 28704. U. M. is supported by the Lee Friedman Memorial Fellowship.

[2] To whom requests for reprints should be addressed, at Department of Medical Physics, Memorial Sloan Kettering Cancer Center, 1275 York Avenue, New York, NY 10021.

[3] The abbreviations used are: NMR, nuclear magnetic resonance; PCr, phosphocreatine; NTP, nucleotide triphosphate; PME, phosphomonoester; PME′, downfield component of PME peak; PC, phosphocholine; PE, phosphoethanolamine; PDE, phosphodiester; GPC, glycerophosphocholine; RIF-1, radiation-induced fibrosarcoma; MCa, mammary carcinoma; *T*1, spin-lattice relaxation constant; FBS, fetal bovine serum; G_{1D}, diploid cells in G_1; G_2-M_T, tetraploid cells in G_2-M, BrdUrd, 5-bromo-2′-deoxyuridine.

[4] J. C. Street, U. Mahmood, C. Matei, and J. A. Koutcher, unpublished results.

increase the magnetic field homogeneity for improved spectral resolution and to maintain tumor temperature, the tumor-bearing portion of the animals was immersed in a water bath at 37°C as described previously (13). A single 9-mm inside diameter four turn Teflon-coated solenoid coil was used for the entire *in vivo* portion of the experiment. No anesthesia was used during spectral acquisitions in order to avoid possible metabolic artifacts (17, 18). The animals were allowed to equilibrate to their new environment for approximately 15 min before phosphorus spectra were acquired. During this time, automatic shimming typically resulted in water proton line widths of 20–30 Hz (0.1–0.15 ppm). Experimental parameters included a spectral width of 10,000 Hz, delay of 2 s, 60-degree spin flip angle, 2048 data points, and 1024 signal averaged free induction decays, resulting in an acquisition time of 34 min/spectrum. To limit possible effects due to $T1$ saturation (19, 20), both *in vivo* and *in vitro* spectra were acquired in the same magnet at the same field strength, with identical flip angles and repetition times, so that the spectra were saturated to approximately the same degree. The free induction decays in both cases were filtered with 5-Hz exponential multiplication; the transformed spectra were manually baseline corrected. Peak heights were used for the analysis of the PME′:PC ratio. Because of the degree of overlap of the PME′ and PC peaks, peak heights have been shown to be more reproducible than deconvolution when analyzing the phosphomonoester region of the spectrum (21). Due to the relatively low signal:noise ratio of the GPC peak, especially *in vivo*, peak heights were also used in calculating the GPC:NTP ratio. The NTP:P_i and PCr:P_i ratios were based on peak area ratios calculated from fitting the resonances to Lorentzian peaks. The β-NTP peak was used to estimate all ratios involving NTP, since the α and γ peaks overlap other resonances. Tumor pH was estimated from the chemical shift of P_i relative to that of PCr (22) using a previously determined calibration curve (23). Because the exact intracellular concentrations of substances which could affect the PCr-P_i chemical shift are not known, the derived pH-chemical shift curve has an uncertainty of ±0.1 pH unit (24). Peak assignments were based on the study of RIF-1 tumors by Evanochko *et al.* (25), except PE is represented as PME′, as noted previously.

***In Vitro* NMR.** RIF-1 cells were grown in monolayer in RPMI 1640 supplemented with 10% FBS (Intragen, Purchase, NY) and penicillin and streptomycin (100 units/ml) in 95%/5% air/CO_2 at 37°C for the *in vitro* portion of the study. To ensure consistency within this study, a single lot of FBS was used, especially to ensure constant levels of ethanolamine (26, 27). RPMI 1640, the medium used throughout these experiments, does not contain ethanolamine, which is entirely supplied by the FBS. Between 50 and 150 × 10^6 cells from four 175-cm^2 Falcon tissue culture flasks (Becton Dickinson, Oxnard, CA) were used per experiment. Cells in the exponential phase of growth were used, since confluency has been shown in other cell lines to increase the phosphodiester region of the spectrum (28) and decrease PE and PC (29). Medium (100 ml/flask) was changed approximately 12 h prior to radiation, and every 36–48 h post radiation.

A modified version of the agarose gel thread technique of Foxall and Cohen (30) was implemented. Cells were trypsinized and centrifuged twice; the cell pellet with approximately 50% additional volume of supernatant was used for extrusion. A 1.8% agarose mixture of low gelling temperature agarose (Sea-Plaque Agarose; FMC BioProducts, Rockland, ME) and RPMI 1640 plus FBS was melted and then cooled to 35°C. It was added in a 1:1 ratio to the cell pellet, which was preheated to 35°C. After passing through 0.5-mm inside diameter Tygon microbore tubing (Cole-Parmer, Niles, IL) placed in an ice bath, the agarose threads were extruded directly into a modified 12-mm NMR tube (Wilmad, Buena, NJ) which contained chilled RPMI 1640 plus FBS.

After extrusion, the cells were continually perfused with phosphate-free RPMI 1640 plus 10% FBS plus penicillin/streptomycin. Phosphate from the fetal bovine serum was sufficient to keep the cells stable (as reflected by stable phosphorus spectra) for more than 24 h. The first 30–40 ml of phosphate-free perfusate went to a waste beaker. This allowed the removal of residual RPMI 1640 and loose cellular debris from the system before the medium was recycled in a closed loop. The media reservoir contained approximately 500 ml phosphate-free medium which was in equilibrium with 95%/5% O_2/CO_2 in the head space. A peristaltic P-3 pump (Pharmacia, Piscataway, NJ) sent media through oxygen-impermeable tubing (No. 13 food grade norprene tubing; Cole-Parmer) to the NMR tube at a rate of 1–2 ml/min. Agarose threads were kept in place by a paper filter (AP prefilter; Millipore, Bedford, MA) supported by a Teflon plug which contained six 1.5-mm holes for media return. Temperature was maintained in the system via a circulating water pump kept at 37°C. Media lines were jacketed; the NMR tube was placed within a double-walled glass beaker (Cole-Parmer) which acted as a heat reservoir. The beaker also helped to improve magnetic field homogeneity via susceptibility matching, as in the *in vivo* experiments (13).

The phosphorus spectra were acquired using a double-tuned (^1H, ^{31}P) coil with parameters similar to the *in vivo* acquisitions: 81.03-MHz resonant frequency, 2-s delay, a spectral width of 10,000 Hz, and a 60-degree spin flip angle. Because of better field homogeneity, 4096 data points were used. Shimming resulted in water proton line widths of approximately 10 Hz. The decreased signal strength compared to the *in vivo* experiment required increased signal averaging. Blocks of 4096 free induction decays (acquisition time, 2.3 h) were added together to improve the signal:noise ratio. Between two and six blocks were added together for analysis after the transformed spectrum of each block was checked for stability. The first 2–3 h after perfusion began were not used for analysis because of transient changes in energy and membrane precursors observed in the spectra, which may have been caused by stress from trypsinization and the extrusion process. Unlike the *in vivo* tumors which were studied serially, each perfusion run yielded data for only one time point, either baseline (no radiation), or at 1, 2, 4, or 7 days post radiation.

Irradiation. Localized *in vivo* irradiation was performed using techniques described previously (1, 3); a single dose of 17 Gy was given when tumors reached a volume of 150–250 mm^3. For the *in vitro* experiments, exponentially growing RIF-1 cells were irradiated at a dose rate of 84.0 cGy/min for 20.3 min using a ^{137}Cs irradiator (Gammacell 40; Atomic Energy of Canada) to expose the cells to a total dose of 17 Gy. The tissue culture flasks were at room temperature for approximately 1 h around the time of irradiation. After irradiation, the cells were returned to the incubator until the time after radiation at which they were to be studied. Because cells do not cycle in the agarose threads (31), reported time points post radiation are from the time of radiation to the time of trypsinization.

Cell Cycle Analysis. For the *in vitro* experiments, an aliquot (0.3 ml) of the cell suspension created by trypsinization at the time of extrusion into agarose threads was placed in 5 ml iced 70% ethanol, vortexed, and stored below 0°C. Staining of cellular DNA and protein content in RIF-1 cells was performed as described previously (32). The RIF-1 cell line has both diploid and tetraploid populations, with the G_2-M fraction of the diploid population overlapping the G_1 fraction of the tetraploid population. Because they do not overlap other peaks *in vitro*, G_{1D} (diploid cells in G_1) and G_2-M_T fractions were used to describe perturbations in cell cycle kinetics.

An additional series of flow cytometry experiments were performed on a parallel set of cultured RIF-1 cells to determine if the sustained increase in the G_2-M_T fraction post radiation was due to a continuing G_2 block or if the length of the cell cycle had substantially increased after irradiation, which could also result in an increased G_2-M_T fraction. Briefly, 13 sets of cells (3 sets each at baseline and 1, 2, and 4 days post radiation and 1 set at 7 days post radiation) were grown and irradiated in culture flasks. The cells were allowed to incorporate BrdUrd for 1 h prior to exposure to UV light. As described previously (33), the cells were harvested, resuspended in tissue culture medium, and illuminated with UV light for 5 min. The strand breaks generated by photolysis of DNA at sites of BrdUrd incorporation were labeled with digoxygenin-conjugated dUTP followed by staining with fluoresceinated antibody to digoxygenin. The percentage of cells incorporating BrdUrd (S-phase cells) was calculated for both ploidy levels for each set of control and post irradiated cultures.

Statistics. All data are reported as mean ± SE. Significance was determined using Student's t test for comparison of the difference between means. Paired t tests were used for the *in vivo* studies, because the mice were followed serially, and unpaired t tests were used for the *in vitro* studies, because each perfusion run yielded data for only one time point.

RESULTS

The RIF-1 tumors implanted in the feet of C3H/He mice have a doubling time of approximately 7 days. For the *in vivo* radiation experiments, a total of 10 tumor-bearing mice were studied serially at five time points. As shown in Fig. 1, the initial tumor volume at

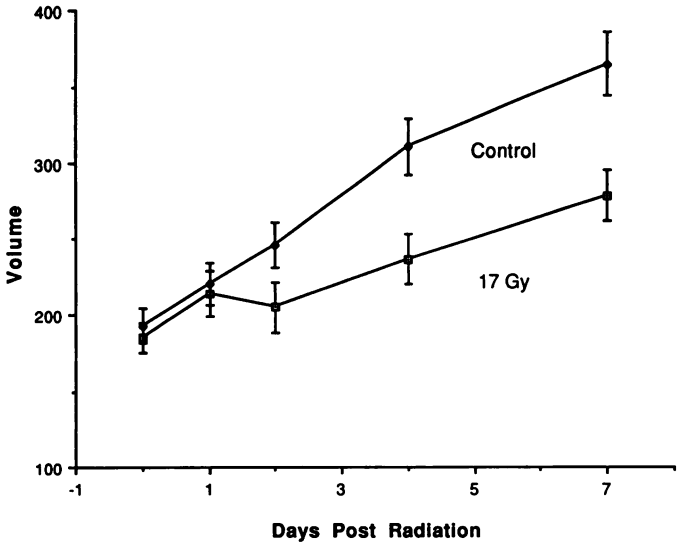

Fig. 1. Volume (in mm^3) of *in vivo* tumors for 7 days post-17 Gy, compared to control tumors which received no radiation. A growth delay of approximately 3.5 days is noted.

baseline was 185 ± 10 mm^3, increased to 214 ± 15 mm^3 at 24 h, and decreased to 205 ± 17 mm^3 at 48 h after 17 Gy, before subsequently increasing again. In comparison, unirradiated RIF-1 tumors started at 193 ± 11 mm^3 and increase to 220 ± 14 mm^3 by 24 h and 246 ± 15 mm^3 by 48 h. The time for the tumors to increase their volume by 50% was 7 days for tumors receiving 17 Gy and approximately 3.5 days for untreated tumors, resulting in a growth delay of approximately 3.5 days. *In vitro*, the RIF-1 cells grown in RPMI 1640 plus 10% FBS in monolayer have a doubling time of approximately 0.6 day. A total of 23 perfusion runs were performed: 6 baseline experiments without radiation; 4 studies each at 24, 48, and 96 h after 17 Gy; and 5 experiments at 168 h post irradiation.

Fig. 2*A* shows spectra serially obtained from a single RIF-1 tumor implanted in a mouse foot, while Fig. 2*B* shows a series of spectra obtained from perfused RIF-1 cells. In contrast to the series of spectra in Fig. 2*A* which are from one mouse, each spectrum for the *in vitro* experiments was obtained from a different set of cells to ensure that spectra from later time points were not affected by the lack of cell cycling in agarose threads or the low phosphate concentration of the perfusate. The cell spectra were stable for more than 24 h, after an initial equilibration of less than 2 h. Spectral changes post irradiation, both *in vivo* and *in vitro*, include an increase in the PME′ peak, composed primarily of phosphoethanolamine, relative to phosphocholine, the upfield component. Increases in glycerophosphocholine are more pronounced *in vitro* than *in vivo*, while changes in energy status are observed in both systems after 17 Gy. Much of the P_i peak *in vitro* is contributed by the perfusate; accurate intracellular and extracellular contributions cannot be readily determined in this system. The overlap of the P_i components suggests that intracellular pH is approximately equal to the pH of the perfusate.

Fig. 3 shows changes in the level of components of the phosphomonoester peak, as reflected by changes in the PME′:PC peak height ratio after irradiation. Both *in vivo* and *in vitro*, PME′:PC significantly increased after 17 Gy compared to control values ($P < 0.005$ for all days post radiation *in vivo*, and $P \leq 0.005$ for days 2–7 post radiation *in vitro*). *In vivo*, PME′:PC increased sharply in the first 24 h and more slowly over the next 3 days, reaching a maximum at day 4, before a small (not statistically significant) decrease from peak values was seen by day 7, the last day studied. In contrast to the changing slope over time seen *in vivo*, PME′:PC continued to increase for the cells irradiated in tissue culture flasks and kept in monolayer post radiation. The increase *in vitro* is linear throughout the 7-day period studied, with a linear correlation coefficient of $r^2 = 1.00$. The absolute difference in the initial values of this ratio *in vivo* and *in vitro* is likely unimportant, inasmuch as the level of the PME′ peak can be changed severalfold for baseline *in vitro* spectra by changing the lot of FBS added to the media (data not shown), probably due to variations in the ethanolamine level between lots (26, 27). The increase *in vitro* in

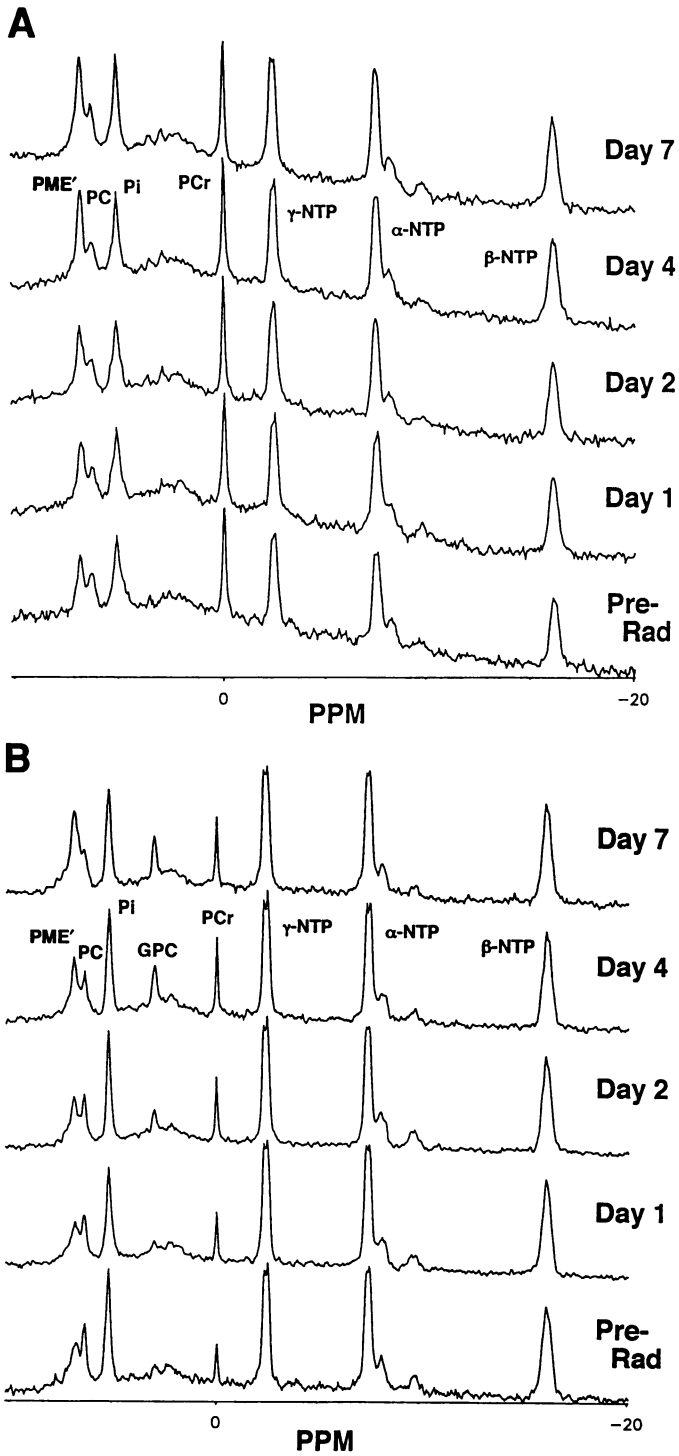

Fig. 2. *A*, serial ^{31}P NMR spectra from a single mouse tumor which received 17 Gy, with peaks as labeled. Note that the phosphomonoester peak is clearly resolved into two components without decoupling. *B*, representative ^{31}P NMR spectra from different sets of RIF-1 cells grown, radiated, and maintained in monolayer. Each set of cells yielded data for one time point only. Time is from radiation until trypsinization for extrusion into agarose threads.

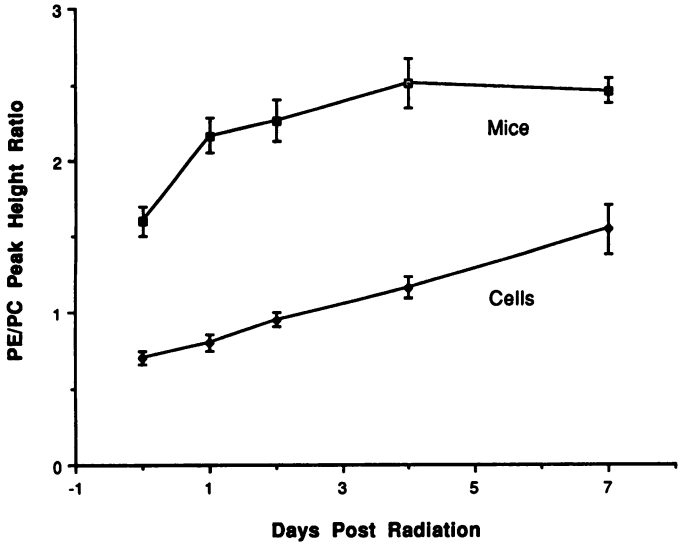

Fig. 3. PME′:PC peak height ratio for the 7 days following a 17-Gy dose. The ratio increases both *in vivo* and *in vitro*, with the *in vitro* PME′:PC ratio increasing linearly (r^2 = 1.00).

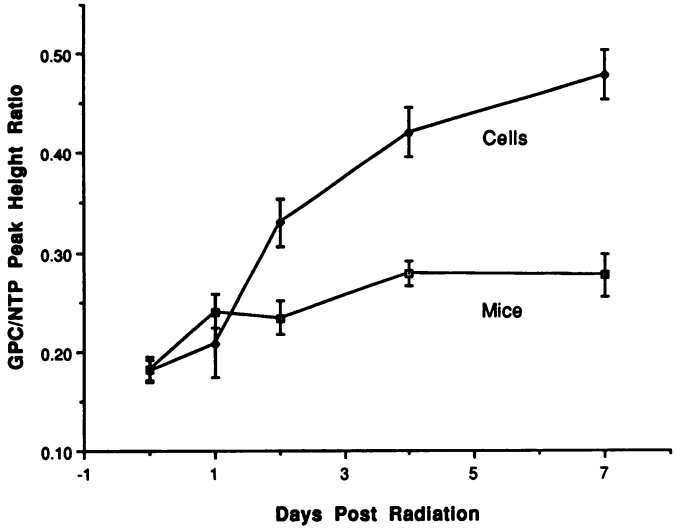

Fig. 4. GPC:NTP peak height ratio after tumors and cells received 17 Gy. Increases in GPC:NTP are significant for both *in vivo* and *in vitro* states, with *in vitro* changes more pronounced. Glycerophosphoethanolamine did not increase above noise levels for any day post radiation either *in vivo* or *in vitro*.

PME′:PC post radiation occurred while an approximately constant level of ethanolamine was provided to the cells through frequent medium changes when the cells were in culture flasks and by the use of a large media reservoir when the cells were perfused in agarose threads. Qualitatively, much of the change in PME′:PC both *in vivo* and *in vitro* appears to be due to post radiation increases in the level of PME′, reflected in increased PME′:NTP ratios, while the level of PC:NTP remained relatively unchanged (data not shown).

Fig. 4 shows changes in the levels of the membrane degradation product glycerophosphocholine, as reflected by changes in the GPC:NTP peak height ratio after irradiation. For the RIF-1 cells grown and maintained with fresh media in culture flasks after radiation, GPC:NTP increased significantly after 17 Gy ($P < 0.001$ for days 2–7 *in vitro*). In RIF-1 tumors in mice, GPC:NTP also increased significantly post radiation ($P < 0.05$ for days 1–2 and $P < 0.01$ for days 4–7 *in vivo*). Although GPC increased both *in vivo* and *in vitro*, the magnitude of the response to radiation is greater for the cultured cells. Glycerophosphoethanolamine in perfused cells and *in vivo* was not consistently detectable above noise level for any of the days studied post radiation. A third peak, approximately 2.0 ppm downfield of PCr, was also located in the phosphodiester region. This peak was small and showed a large degree of variability; no changes in peak height with respect to time post radiation were noted *in vivo* or *in vitro* at this location.

Fig. 5*A* shows the changes in PCr:P_i and NTP:P_i peak area ratios of the *in vivo* tumors post radiation. The energy status of the tumors reaches a maximum 1–2 days after radiation, as reflected by these ratios. Statistically significant increases over baseline values were observed for day 1 ($P \leq 0.01$ for NTP:P_i), day 2 ($P \leq 0.001$ for NTP:P_i; $P \leq 0.05$ for PCr:P_i), and day 4 ($P \leq 0.01$ for NTP:P_i) after 17 Gy. Fig. 5*B* shows the changes in the PCr:NTP peak area ratio in perfused cells. Since intracellular P_i could not be determined, PCr:P_i and NTP:P_i could not be calculated for the *in vitro* study; however, PCr:NTP may also reflect changes in energy status (7). The cellular energy, as reflected by the PCr:NTP ratio, showed an increase, compared to controls, at day 2 ($P < 0.001$) and remained elevated at day

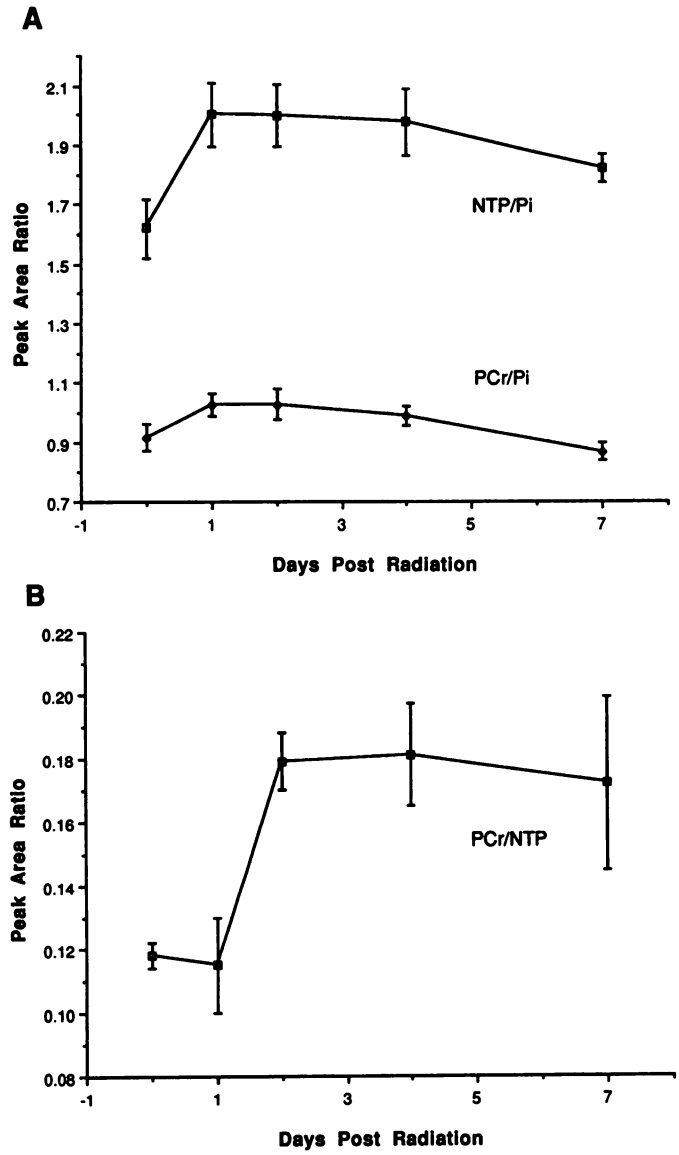

Fig. 5. *A*, *in vivo* energy status of tumors post-17 Gy, as represented by PCr:P_i and NTP:P_i peak area ratios. *B*, *in vitro* energy status of perfused cells post-17 Gy, as represented by the PCr:NTP peak area ratio.

4 ($P < 0.002$) and day 7 post radiation for the *in vitro* study. Therefore, the temporal pattern of post radiation energy changes is different *in vivo* and *in vitro*. The *in vivo* NTP:P_i and PCr:P_i ratios peaked 1–2 days after radiation and monotonically decreased thereafter. In contrast, the *in vitro* energy status was unchanged 24 h after radiation and then increased to an elevated level, where it remained between days 2 and 7 post radiation.

In contrast to the energy status response to radiation, the *in vivo* pH did not change after receiving 17 Gy. The pH at baseline and on days 1, 2, and 7 post radiation was 7.18 ± 0.01; the pH on day 4 was 7.19 ± 0.01. The baseline pH is similar to values reported for the RIF-1 tumor at other sites (7, 9, 10), which suggests that the dorsal aspect of the foot results in adequate perfusion for tumors in the size range studied (150–250 mm^3). The mean pH for the 23 perfusion experiments was 7.27 ± 0.01, which represents a weighted average of the media and cellular pH, inasmuch as these were not resolved.

To ensure that post radiation changes in the ratios presented in the current study were not a result of relative changes in *T*1s, 4 perfusion experiments, 2 without radiation and 2 at 96 h post-17 Gy, were performed with both 2- and 10-s repetition times. Qualitatively, PME′ and PC appear to have similar *T*1 relaxation rates, both before and after radiation; *i.e.*, the $T1_{PME'}:T1_{PC}$ ratio does not change after radiation. Although GPC has a longer *T*1 than NTP, the relative increase in GPC:NTP for 10 s compared to 2 s repetition time is unaffected by radiation. Similarly, the *T*1 effects upon PCr:NTP qualitatively appear unchanged after radiation for a repetition time of 2 s. The temporal responses of the ratios calculated in this study are therefore not due to changes in relaxation times.

Fig. 6 shows representative cell cycle distributions for cultured cells prior to and 2 days after receiving 17 Gy. There was an increase compared to baseline in the G_2-M tetraploid fraction starting 1 day after radiation. The elevation in the G_2-M_T fraction was sustained throughout the 7-day period studied. At baseline, the G_2-M_T fraction started at 8.4 ± 0.8% and increased on day 1 post radiation to 40.3 ± 3.7%. On day 2 post-17 Gy the G_2-M_T fraction was 35.0 ± 2.4%, on day 4 it was 39.7 ± 2.1%, and on day 7 post radiation it was 41.7 ± 1.6%. The increase in G_2-M_T compared to baseline values is significant for all of the post radiation days studied ($P < 0.001$). The difference among post radiation G_2-M_T values is not significant.

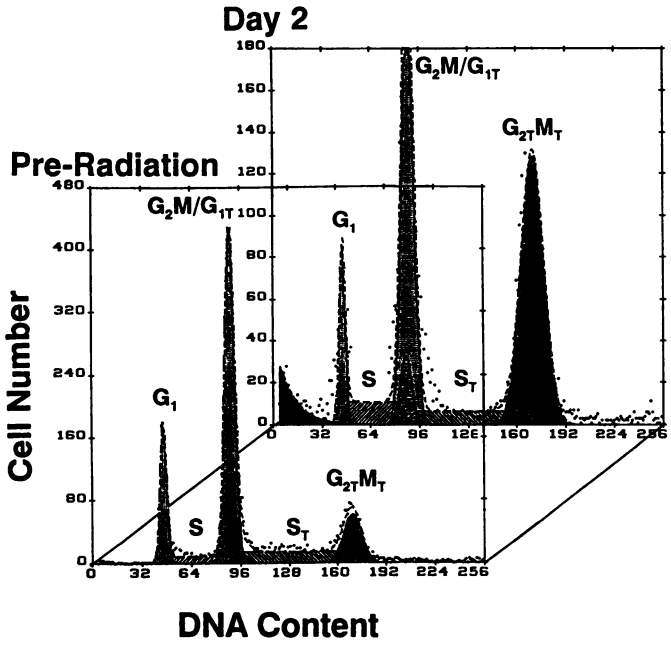

Fig. 6. Representative flow cytometry data, showing both unirradiated cells and cells that were irradiated 2 days previously. The percentage of cells in G_2-M increases by 24 h post-17 Gy and remains elevated for at least 7 days after irradiation in culture.

BrdUrd incorporation observed in a parallel series of experiments revealed that the diploid (S_D) and tetraploid (S_T) S phase fractions decreased from approximately 13.0 and 19.0%, respectively, in the pretreatment samples to less than 2.0 and 3.0%, respectively, in samples from 1–7 days post irradiation. In each instance, a proportion of S-phase cells failed to incorporate BrdUrd, indicating that their progression through S phase had slowed to such an extent that they could be considered noncycling. The fraction of noncycling or quiescent S-phase cells increased from approximately 3% for both ploidies in pretreatment cultures to 4–8% and 8–15%, respectively, for the S_D and S_T cell populations with increasing time in culture following irradiation.

The degree of dUTP incorporation is expected to be proportional to the rate of S phase traverse when the length of exposure to BrdUrd is kept constant. In experiments performed at various times following irradiation, the mean dUTP incorporation among cycling cells decreased substantially with time: for the S_D population on Day 1, 2, and 4 following irradiation the mean dUTP incorporation values fell to 96, 76, and 53% of pretreatment values, respectively; while for the S_T populations the values were 98, 81, and 60%, respectively, at the same time points. The decreased level of incorporation indicates a slowdown in S phase traverse.

DISCUSSION

In order to elucidate which post radiation changes, including increases in PME′:PC, increases in GPC:NTP, and increases in energy status, seen in the *in vivo* ^{31}P NMR spectra are direct cellular effects and which changes are a result of systemic alterations, we have observed the effects of 17 Gy of radiation on murine RIF-1 tumors, both in the mouse foot and grown and radiated in monolayer with subsequent artificial perfusion in an agarose gel thread system. Flow cytometry data were also obtained from the cultured cells to correlate NMR changes with changes in cell cycle. Other investigators have compared untreated *in vitro* phosphorus spectra obtained using a variety of perfusion methods to the same human cell lines grown *in vivo* in nude mice (28, 34–36). Another group has also investigated changes after radiation in the RIF-1 line, *in vivo* in the mouse flank for 300-mm^3 tumors (9) and *in vitro*, with perfusion and radiation of cells in calcium alginate beads (12).

Membrane Phospholipid Precursors. Fig. 3 shows changes in the phosphomonoesters after radiation. Both *in vivo* and *in vitro*, PME′:PC increases post-17 Gy, with a linear increase seen *in vitro*. The similar pattern of increase in the PME′:PC ratio for implanted tumors and for cells grown in tissue culture indicates that these changes are due to an inherent cellular effect. The smaller differences in the temporal response between the *in vivo* and *in vitro* states may be due to a modulation of the intrinsic response by systemic effects, such as blood flow or hormonal changes, or to a different temporal response from stromal cells, which can comprise 50% of the cells in a solid tumor. The results presented here for the *in vivo* RIF-1 tumor model are qualitatively very similar to results we have obtained previously from MCa tumors implanted in C3H/He mice (1, 2, 8). In those studies, PME′:PC peaked approximately 7 days post-8, -17, -32, and -65 Gy.

Freyer *et al.* (37) studied EMT6/Ro spheroids over a wide size range and observed that PE:PC had a significant negative correlation with the S-phase fraction. In a study of four perfused cell lines, Scherer *et al.* (38) noted that, independent of cell density, low PE levels were associated with rapid cell division and that these levels

markedly increased when growth stopped. Both of these studies are consistent with the concomitant increase in the PME′:PC ratio and the G_2 block seen post radiation in the RIF-1 line, and with our earlier data indicating similar changes in phosphomonoesters after tumoricidal doses of radiation in the MCa tumor model (1, 2, 8).

Membrane Phospholipid Catabolites. Glycerophosphocholine was observed to increase significantly relative to NTP post radiation, with a greater increase *in vitro* than *in vivo*, as shown in Fig. 4. Glycerophosphoethanolamine was not consistently detected above the level of background noise for any day post irradiation in either system. In an *in vivo* study of an estrogen-sensitive tumor by Smith *et al.* (39), the concentration of GPC was negatively correlated with both the percentage of cells synthesizing DNA and the percentage of cells in S phase. The changes in that work are consistent with our experiments which showed increases *in vitro* in GPC and the G_2-M_T population post radiation. However, several studies do not support these findings. In their study of EMT6/Ro spheroids, Freyer *et al.* (37) found no correlation between GPC:P_i and S-phase fraction. Vijayakumar *et al.* (31) observed no significant changes in the amount of GPC in perfused carcinoma cells during the 2 days post-50 Gy studied, despite increases in the G_2-M population during this time. Majors *et al.* (11) detected no significant changes in the PDE region after 14 Gy during the 3 days over which tumors implanted on the flank were followed post radiation. Spectral noise or the wide range of sizes used in that work (200–800 mm^3) may have concealed subtle radiation-induced changes in GPC concentration.

The increase in GPC:NTP after irradiation both for RIF-1 tumors and cultured cells indicates that these effects are direct cellular events that are being monitored by NMR and are not due to systemic effects such as changes in blood flow. The overall decreased response *in vivo* compared to that seen in the cultured cell system may reflect an increased washout of GPC *in vivo*, a dilution of the effect by normal stromal cells within the tumor, or a decreased production of GPC post radiation due to the three-dimensional architecture found *in vivo*, compared to the two-dimensional structure *in vitro*.

With respect to phospholipid precursors and catabolites, the two primary changes in the RIF-1 post radiation are the increase in PME′:PC and the increase in GPC:NTP both *in vivo* and *in vitro*. As suggested previously (1, 2, 8), a number of possible intrinsic cellular mechanisms are consistent with the *in vitro* findings. Membranes could suffer direct radiation damage, resulting in increased catabolism via phospholipases. The radiation-induced G_2 block may also alter membrane precursor and catabolite concentrations, through a decreased demand for new membrane synthesis or other secondary effect. Radiation-induced DNA damage could also affect enzyme activity by altering gene expression. In the MCa tumor model, the ratio of phospholipids that contain ethanolamine compared to those that contain choline increases significantly by 96 h after a 32- or 65-Gy radiation dose (40). The changes seen in the phospholipid precursors and catabolites post radiation may therefore reflect changes in the phospholipids themselves. Because of the numerous pathways which change the levels of PMEs and PDEs, mechanistic causes based upon the experiments performed in this study cannot be assigned. ^{13}C NMR experiments using isotopically labeled choline and ethanolamine may help further define the basis of the alterations observed in the ^{31}P NMR spectra post radiation.

Energy Changes. The energy changes after radiation differ qualitatively in their temporal course *in vitro* and *in vivo*, as shown in Fig. 5. *In vitro* PCr:NTP does not begin to increase until 48 h after radiation and remains at the elevated level on days 4 and 7. In contrast, *in vivo*, both NTP:P_i and PCr:P_i increase 24 h after radiation, peak at 24 to 48 h post-17 Gy, and subsequently decrease through day 7. Previous *in vivo* tumor studies have shown similar increases in energy status which peaked between 1 and 7 days post radiation for doses ranging from 8 to 70 Gy (1, 2, 8–11, 23), although other studies (41, 42) have noted a decrease in the NTP:P_i ratio.

The *in vitro* result of increased energy status after radiation differs from the results obtained by two other groups who examined the effects of radiation on perfused cells. Ng *et al.* (12) followed RIF-1 cells for 60–72 h after radiation. In their system, they initially observed that for both control and radiated cells, there was an increase in the levels of PCr and NTP, which subsequently fell starting at 24 to 30 h after cells were given 15 or 25 Gy but remained elevated for cells given 0 or 10 Gy. In contrast to the current perfusion experiments, the data were obtained from cells irradiated immediately after or immediately prior to extrusion into calcium alginate beads. Data for later time points were obtained from cells which had remained in the beads without undergoing cell division and which had an increase in the G_0/G_1 fraction for nonradiated controls. Perfusion for 3 days with media that was phosphate free except for that derived from the 10% FBS added may have also affected cellular energy. It was noted that only 60–70% of the cells which received 15 or 25 Gy were recovered 30–40 h after perfusion began. For the *in vitro* experiments performed in our study, cells were irradiated in monolayer and were not trypsinized until the time of observation, which was at least 24 h after receiving the 17-Gy dose. Each perfusion run yielded data for only one time point, in order to eliminate the effects on later time points of the lack of cell cycling, low phosphate perfusion media, or other possible effects from the increased cell density. In a study on two human squamous cell carcinoma lines perfused in both basement membrane and agarose threads, Vijayakumar *et al.* (31) detected no significant changes after 2 or 50 Gy in the levels of energy metabolites compared to cells which received no radiation. The contrary results could be due to differences in dose, duration of the experiment, or cell type.

Alterations in the cell cycle distribution post radiation may contribute to intrinsic cellular changes in energy. As represented in Fig. 6, *in vitro* the fraction of cells in G_2-M_T increased after radiation from $8.4 \pm 0.8\%$ to $40.3 \pm 3.7\%$ by 24 h and remained elevated throughout the 7-day period. Wolloch *et al.* (43) have also observed a sustained elevation in the G_2 phase *in vitro* between 1 and 7 days post-10 and -15 Gy for an ovarian carcinoma line. Skog *et al.* (44) noted energy requirements for Ehrlich ascites cells peaked in early G_1. Fed plateau V-79 Chinese hamster cells were shown by Freyer *et al.* (45) to consume one-fifth of the oxygen that exponential cells used. A decrease in the demand for energy in RIF-1 cells post radiation would increase cellular energy reserves, stored as PCr, if energy production remained constant. Cells receiving a sterilizing dose of radiation may expend less energy for tasks such as protein synthesis, which has been shown to use about one-third of the total energy utilized during one cell cycle (44). The initial change in the G_2-M_T fraction is followed 24 h later by the initial change in PCr:NTP, which *in vitro* remains elevated for days 2–7 after irradiation. This suggests that the improved energy status is likely due to decreased utilization of energy.

Conclusions. RIF-1 tumors implanted in the feet of C3H/He mice exhibit a small growth delay after 17 Gy. The PME peak is resolved without decoupling both *in vivo* an *in vitro* into two components, PME′, representing PE and minor contributions from other phosphomonoesters, and PC. The increases in the PME′:PC ratio after irradiation are similar *in vivo* and *in vitro*. The changes post-17 Gy in the GPC:NTP ratio also show similarities between the two states, although a greater increase *in vitro* than *in vivo* is noted. These changes are at the cellular level and are likely due to cell death or growth inhibition after radiation. This is supported by cell cycle data which show a longer S phase traverse and an increased percentage of cells in G_2-M_T. Membrane damage may also directly or indirectly

contribute to the observed alterations in the PME and PDE regions of the phosphorus NMR spectrum.

RIF-1 tumors post irradiation show improvement in their energy status: *in vivo*, a maximum is reached 1–2 days after treatment, before a subsequent decline; *in vitro*, the energy status increases on day 2 post radiation, after which it plateaus. The *in vitro* effects are likely due to a decreased energy demand secondary to a G_2 block. However, based on the substantially different temporal responses *in vivo* and *in vitro*, the energy status changes seen in solid tumors after irradiation are dominated by systemic effects, such as changes in perfusion, with smaller contributions from directly radiation-altered cellular physiology. These interpretations based upon the RIF-1 tumor model located on the feet of C3H/He mice must be verified for other cell lines, tumor volumes, and locations, as relative contributions of host *versus* cellular response may vary among these parameters.

ACKNOWLEDGMENTS

We thank Drs. Pat Faustino and Jack Cohen for their help with the perfusion system.

REFERENCES

1. Koutcher, J. A., Alfieri, A. A., Devitt, M. L., *et al.* Quantitative changes in tumor metabolism, partial pressure of oxygen and radiobiological oxygenation status post radiation. Cancer Res., *52:* 4620–4627, 1992.
2. Mahmood, U., Alfieri, A. A., Thaler, H., Cowburn, D., and Koutcher, J. A. Radiation dose-dependent changes in tumor metabolism measured by ^{31}P nuclear magnetic resonance spectroscopy. Cancer Res., *54:* 4885–4891, 1994.
3. Koutcher, J. A., Alfieri, A. A., Kornblith, A. B., *et al.* Changes in radiation sensitization induced by fluosol-DA as measured by ^{31}P nuclear magnetic resonance spectroscopy. Cancer Res., *50:* 7252–7256, 1990.
4. Daly, P. F., and Cohen, J. S. Magnetic resonance spectroscopy of tumors and potential *in vivo* clinical applications: a review. Cancer Res., *49:* 770–779, 1989.
5. Glickson, J. D., Evanochko, W. T., Sakai, T. T., and Ng, T. C. *In vivo* NMR spectroscopy of tumors. *In:* R. K. Gupta (ed.), NMR Spectroscopy of Cells and Organisms, Vol. 1, pp. 99–134. Boca Raton, FL: CRC Press, 1987.
6. Ng, T. C., Majors, A. W., Vijayakumar S., *et al.* Human neoplasm pH and response to radiation therapy: P-31 MR spectroscopy studies *in situ*. Radiology, *170:* 875–878, 1989.
7. Evelhoch, J. L., Sapareto, S. A., Nussbaum, G. H., and Ackerman, J. J. H. Correlations between ^{31}P NMR spectroscopy and ^{15}O perfusion measurements in the RIF-1 murine tumor *in vivo*. Radiat. Res., *106:* 122–131, 1986.
8. Koutcher, J. A., Alfieri, A. A., Devitt, M. L., Kornblith, A. B., and Cowburn D. Radiation induced ^{31}P NMR spectral changes in a hypoxic tumor: possible association with *in situ* reoxygenation. *In:* Ninth Annual Meeting of the Society of Magnetic Resonance in Medicine, New York, NY, August 18–24, 1990, p. 1261.
9. Rajan, S. S., Wehrle, J. P., Li, S., Steen, R. G., and Glickson, J. D. ^{31}P NMR spectroscopic study of bioenergetic changes in radiation-induced fibrosarcoma-1 after radiation therapy. NMR Biomed., *2:* 165–171, 1989.
10. Tozer, G. M., Bhujwalla, Z. M., Griffiths, J. R., and Maxwell, R. J. Phosphorus-31 magnetic resonance spectroscopy and blood perfusion of the RIF-1 tumor following X-irradiation. Int. J. Radiat. Oncol. Biol. Phys., *16:* 155–164, 1989.
11. Majors, A. W., Ng, T. C., Karalis, I. M., *et al.* Phosphorus metabolites and the distribution of cell cycle phase of RIF-1 tumors in response to 14 Gy irradiation. Magn. Reson. Med., *16:* 425–430, 1990.
12. Ng, C. E., McGovern, K. A., Wehrle, J. P., and Glickson, J. D. ^{31}P NMR spectroscopic study of the effects of γ-irradiation on RIF-1 tumor cells perfused *in vitro*. Magn. Reson. Med., *27:* 296–309, 1992.
13. Ballon, D., Mahmood, U., Jakubowski, A., and Koutcher, J. A. resolution enhanced NMR spectroscopy in biological systems via magnetic susceptibility matched sample immersion chambers. Magn. Reson. Med., *30:* 754–758, 1993.
14. Twentyman, P. R., Brown, J. M., Gray, J. W., Franko, A. J., Scoles, M. A., and Kallman, R. F. A new mouse tumor model system (RIF-1) for comparison of end-point studies. J. Natl. Cancer Inst., *64:* 595–604, 1980.
15. Koutcher, J. A., Barnett, D., Kornblith, A. B., Cowburn, D., Brady, T. J., and Gerweck, L. E. Relationship of changes in pH and energy status to hypoxic cell fraction and hyperthermia sensitivity. Int. J. Radiat. Oncol. Biol. Phys., *18:* 1429–1435, 1990.
16. Koutcher, J. A., Alfieri, A. A., Barnett, D. C., Cowburn, D. C., Kornblith, A. B., and Kim, J. H. Changes in ^{31}P nuclear magnetic resonance with tumor growth in radioresistant and radiosensitive tumors. Radiat. Res., *121:* 312–319, 1990.
17. Zhao, M., Fortan, L. G., Raman, J., Simpson, N. E., and Evelhoch, J. L. Effects of isoflurane on tumor energy metabolism and blood flow in subcutaneous RIF-1. *In:* Twelfth Annual Meeting of the Society of Magnetic Resonance in Medicine, New York, NY, August 14–20, 1993, p. 20.
18. Okunieff, P., Rummeny, E., Vaupel, P., *et al.* Effects of pentobarbital anesthesia on the energy metabolism of murine tumors studied by *in vivo* ^{31}P nuclear magnetic resonance spectroscopy. Radiat. Res., *115:* 361–372, 1988.
19. Li, S., Jin, G., and Moulder, J. E. Effects of local irradiation on spin-lattice relaxation time of phosphate metabolites in mouse tumors monitored by ^{31}P magnetic resonance spectroscopy. Magn. Reson. Med., *23:* 302–310, 1992.
20. Okunieff, P., Ramsay, J., Tokuhiro, T., *et al.* Estimation of tumor oxygenation and metabolic rate using ^{31}P MRS: correlation of longitudinal relaxation with tumor growth rate and DNA synthesis. Int. J. Radiat. Oncol. Biol. Phys., *14:* 1185–1195, 1988.
21. Daly, P. F., Zugmaier, G., Sandler, D., Carpen, M., Myers, C. E., and Cohen, J. S. Regulation of the cytidine phospholipid pathways in human cancer cells and effects of 1-β-D-arabinofuranosylcytosine: a noninvasive ^{31}P nuclear magnetic resonance study. Cancer Res., *50:* 552–557, 1990.
22. Moon, R. B., and Richards, J. H. Determination of intracellular pH by ^{31}P magnetic resonance. J. Biol. Chem., *248:* 7276–7278, 1973.
23. Koutcher, J. A., Okunieff, P., Neuringer, L., Suit, H., and Brady, T. Size dependent changes in tumor phosphate metabolism after radiation therapy as detected by ^{31}P NMR spectroscopy. Int. J. Radiat. Oncol. Biol. Phys., *13:* 1851–1855, 1987.
24. Roberts, J. K. M., Wade-Jardetzky, N., and Jardetzky, O. Intracellular pH measurements by ^{31}P nuclear magnetic resonance. Influence of factors other than pH on ^{31}P chemical shifts. Biochemistry, *20:* 5389–5394, 1981.
25. Evanochko, W. T., Sakai, T. T., Ng, T. C., *et al.* NMR study of *in vivo* RIF-1 tumors: analysis of perchoric acid extracts and identification of ^{1}H, ^{31}P and ^{13}C resonances. Biochim. Biophys. Acta, *805:* 104–116, 1984.
26. Ronen, S. M., Rushkin, E., and Degani, H. Lipid metabolism in T47D human breast cancer cells: ^{31}P and ^{13}C-NMR studies of choline and ethanolamine uptake. Biochim. Biophys. Acta, *1095:*35–16, 1991.
27. Vance, D. E. Phospholipid metabolism and cell signalling in eucaryotes. *In:* D. E. Vance (ed.), Biochemistry of Lipids, Lipoproteins and Membranes, pp. 205–240. New York: Elsevier Science Publishing Co., Inc., 1991.
28. Macdonald, J. M., Kurhanewicz, J., Dahiya, R., *et al.* Effect of glucose and confluency on phosphorus metabolites of perfused human prostatic adenocarcinoma cells as determined by ^{31}P MRS. Magn. Reson. Med., *29:* 244–248, 1993.
29. Daly, P. F., Lyon, R. C., Faustino, P. J., and Cohen J. S. Phospholipid metabolism in cancer cells monitored by ^{31}P NMR spectroscopy. J. Biol. Chem., *262:* 14875–14878, 1987.
30. Foxall, D. L., and Cohen, J. S. NMR studies of perfused cells. J. Magn. Reson., *52:* 346–349, 1983.
31. Vijayakumar, S., Czerski, L., Majors, A., *et al.* Phosphorous metabolite and cell cycle kinetic response of two human squamous cell cycle carcinomas to radiation. Cancer Res., *52:* 5299–5306, 1992.
32. Darzynkiewicz, Z., Williamson, B., Carswell, E. A., and Old, L. J. Cell-cycle specific effects of tumor necrosis factor. Cancer Res., *44:* 83–90, 1984.
33. Li, X., Traganos, F., Melamed, M. R., and Darzynkiewicz, Z. Detection of 5-bromo-2-deoxyuridine incorporated into DNA by labeling strand breaks induced by photolysis (SBIP). Int. J. Oncol., *4:* 1157–1161, 1994.
34. Singer, S., Okunieff, P., Gostin, C., Thilly, W. G., Chen, L. B., and Neuringer, L. J. ^{13}C- and ^{31}P-NMR studies of human colon cancer *in-vitro* and *in-vivo*. Surg. Oncol., *2:* 7–18, 1993.
35. Lyon, R. C., Tschudin, R. G., Daly, P. F., and Cohen, J. S. A versatile multinuclear probe design for *in vivo* NMR spectroscopy: applications to subcutaneous human tumors in mice. Magn. Reson. Med., *6:* 1–14, 1988.
36. Daly, P. F., Lyon, R. C., Straka, E. J., and Cohen, J. S. ^{31}P-NMR spectroscopy of human cancer cells proliferating in a basement membrane gel. FASEB J., *2:* 2596–2604, 1988.
37. Freyer, J. P., Schor, P. L., Jarrett, K. A., Neeman, M., and Sillerud, L. O. Cellular energetics measured by phosphorous nuclear magnetic resonance spectroscopy are not correlated with chronic nutrient deficiency in multicellular tumor spheroids. Cancer Res., *51:* 3831–3837, 1991.
38. Scherer, P. G., Galons, J., McGovern, K. A., Okerlund, L. S., and Gillies, R. J. Phosphomonoesters and growth in cultured cells. *In:* Society of Magnetic Resonance in Medicine, 10th Annual Meeting, San Francisco, CA, August 10–16, 1991, p. 1078.
39. Smith, T. A. D., Eccles S, Ormerod, M. G., Tombs, A. J., Titley, J. C., and Leach, M. O. The phosphocholine and glycerophosphocholine content of an oestrogen-sensitive rat mammary tumour correlates strongly with growth rate. Br. J. Cancer, *64:* 821–826, 1991.
40. Merchant, T. E., Alfieri, A. A., Glonek, T., and Koutcher. J. A. Comparison of relative changes in phosphatic metabolites and phospholipids following irradiation. Radiat. Res., in press, 1995.
41. Kristjansen, P. E. G., Pedersen, E. J., Quistorff, B., Elling, F., and Spang-Thomsen, M. Early effects of radiotherapy in small cell lung cancer xenografts monitored by ^{31}P magnetic resonance spectroscopy and biochemical analysis. Cancer Res., *50:* 4880–4884, 1990.
42. Sijens, P. E., Bovee, W. M. M. J., Seijkens, D., Los, G., and Rutgers, D. H. *In vivo* ^{31}P-nuclear magnetic resonance study of the response of a murine mammary tumor to different doses of γ-radiation. Cancer Res., *46:* 1427–1432, 1986.
43. Wolloch, E. H., Sevin, B. U., Perras, J. P., *et al.* Cell kinetic perturbations after irradiation and caffeine in the BG-1 ovarian carcinoma cell line. Gynecol. Oncol., *43:* 29–36, 1991.
44. Skog, S., Tribukait, B., and Sundius, G. Energy metabolism and ATP turnover time during the cell cycle of Ehrlich ascites tumour cells. Exp. Cell Res., *141:* 23–29, 1982.
45. Freyer, J. P., Tustanoff, E., Franko, A. J., and Sutherland, R. M. *In situ* oxygen consumption rates of cells in V-79 multicellular spheroids during growth. J. Cell. Physiol., *118:* 53–61, 1984.